

Tearing of metallic sandwich panels subjected to air shock loading

Feng Zhu

*Faculty of Engineering and Industrial Sciences, Swinburne University of Technology,
John Street, Hawthorn, VIC 3122, Australia*

Guoxing Lu[†]

*Faculty of Engineering and Industrial Sciences, Swinburne University of Technology,
John Street, Hawthorn, VIC 3122, Australia
School of Mechanical and Aerospace Engineering, Nanyang Technological University,
50 Nanyang Avenue, Singapore 639798*

Dong Ruan

*Faculty of Engineering and Industrial Sciences, Swinburne University of Technology,
John Street, Hawthorn, VIC 3122, Australia*

Dongwei Shu

*School of Mechanical and Aerospace Engineering, Nanyang Technological University,
50 Nanyang Avenue, Singapore 639798*

(Received November 29, 2008, Accepted February 20, 2009)

Abstract. This paper presents a computational study for the structural response of blast loaded metallic sandwich panels, with the emphasis placed on their failure behaviours. The fully-clamped panels are square, and the honeycomb core and skins are made of the same aluminium alloy. A material model considering strain and strain rate hardening effects is used and the blast load is idealised as either a uniform or localised pressure over a short duration. The deformation/failure procedure and modes of the sandwich panels are identified and analysed. In the uniform loading condition, the effect of core density and face-sheets thicknesses is analysed. Likewise, the influence of pulse shape on the failure modes is investigated by deriving a pressure-impulse (P-I) diagram. For localised loading, a comparative study is carried out to assess the blast resistant behaviours of three types of structures: sandwich panel with honeycomb core, two face-sheets with air core and monolithic plate, in terms of their permanent deflections and damage degrees. The finding of this research provides a valuable insight into the engineering design of sandwich constructions against air blast loads.

Keywords: sandwich panel; blast loading; numerical simulation; P-I diagram; failure modes.

[†] Corresponding author, E-mail: gxlu@ntu.edu.sg

1. Introduction

As a novel and promising energy absorber, sandwich structures have been increasingly applied in the areas of impact and blast protection, such as ship, aircraft, automotive and aerospace industries, packaging and construction engineering. A typical sandwich construction usually consists of two metallic face-sheets and a core made from compressible cellular solids (frequently honeycomb or metallic foam). During an impact, on one hand, the kinetic energy can partially be absorbed by bending and stretching of the plate, which is a global response of the whole structure; on the other hand, a large amount of the impact energy is dissipated by the plastic collapse of sandwich core, which deforms locally. The face-sheets can provide the structure with higher bending and stretching strengths, while the local indentation is dominated by the behaviour of the core material, which becomes crushed as transverse stress becomes large. The impact response of sandwich structure has been extensively studied over the past decade, and comprehensive reviews can be seen in (Abrate 1989, Lu and Yu 2003).

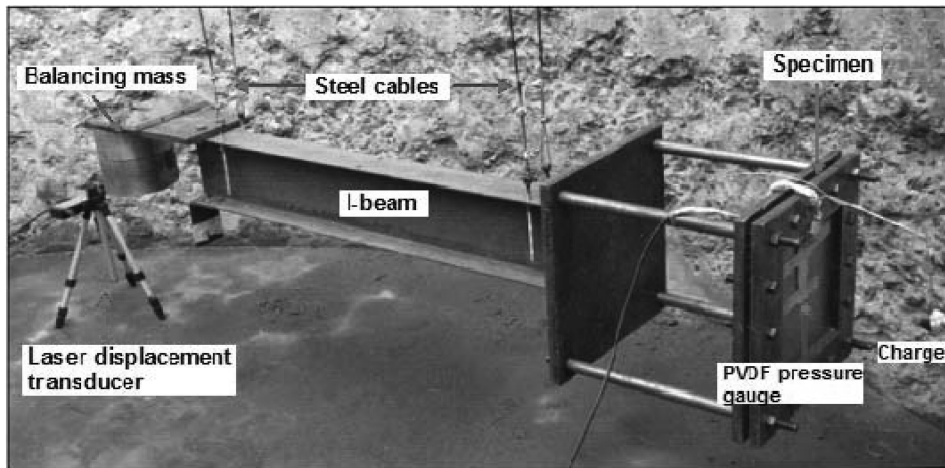
In recent years, more attention has been turned to the performance of such structures under blast loading due to the enhanced chance of accidents or terroristic attacks. The blast response of sandwich structures, however, has been less reported to date. The early works were focused on the analytical and numerical modelling of sandwich beams (Fleck and Deshpande 2004, Qiu *et al.* 2003, Xue and Hutchinson 2004, Hutchinson and Xue 2005) and circular plates (Qiu 2004, Xue and Hutchinson 2003). More recently, Dharmasena *et al.* (2008) reported a small number of blast tests on square sandwich panels, together with a simple numerical simulation. Zhu *et al.* conducted a systematic experimental (Zhu *et al.* 2008a), numerical (Zhu *et al.* 2009b, 2008b) and analytical investigation (Zhu *et al.* 2009a, 2009c) on the fully clamped rectangular sandwich panels with either a honeycomb core or an aluminium foam core. In all the above studies, the responses concerned mainly include the permanent deflection of the structure, reaction forces at the supports and energy absorption etc; no structural damage (e.g. tearing or rupture) has been considered. In other words, the separation of material was not taken into account. In practice, however, structural damage may take place frequently when subjected to intense loads such as blasting. Vaziri *et al.* (2007) assessed the failure behaviours of steel sandwich beams with either square honeycomb core or folded plate core via numerical simulations. Effect of material properties such as strength, strain hardening and ductility on the necking and subsequent tearing was emphasised. No detailed parametric studies on the influence of structure configurations and loading conditions were reported.

Based on FE modelling as well, this paper presents a detailed analysis on the failure modes of square aluminium sandwich panels with a hexagonal honeycomb core, in the viewpoint of structural specifications and loading conditions. The experimental setup and procedure were reported in (Zhu *et al.* 2008a) and they are briefly reviewed in Section 2. Section 3 then gives the details of the numerical model. Two loading conditions, i.e. uniform loading and localised loading, are discussed in Sections 4 and 5, respectively. In both cases, the failure procedure and modes of a typical sandwich panel are described. For uniform loading, effect of two key design parameters, that is, core density and face thickness, is analysed; the influence of pulse shape is studied using a pressure-impulse diagram. In the case of localised loading, on the other hand, a parametric study is conducted for three cases: a sandwich panel with honeycomb core, two faces with air core and a monolithic plate.

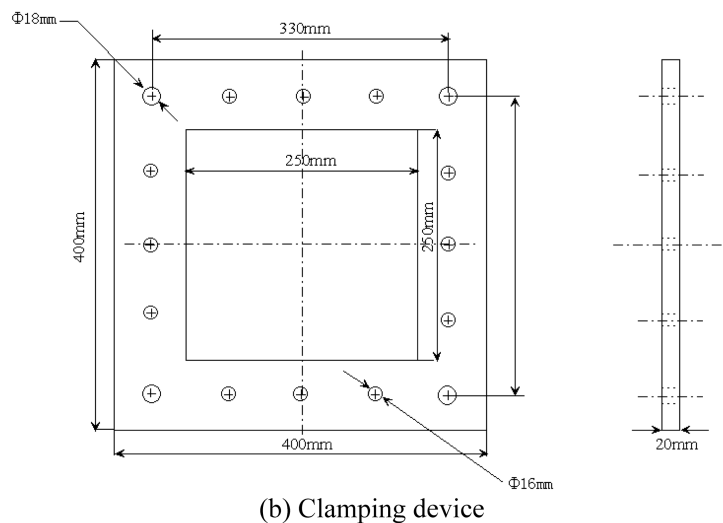
2. Experiment

The setup and procedure of the blast tests are briefly reviewed in this section. The detailed description of experimental procedure, results and parametric studies can be seen in (Zhu *et al.* 2008a,b, 2009a,b,c).

A four-cable ballistic pendulum system has been employed to measure the impulse delivered on the pendulum and specimen. Fig. 1(a) shows the pendulum set-up. The specimens were peripherally clamped between two square steel frames, as shown in Fig. 1(b). The frames were screwed on the front face of the pendulum, and the charge was fixed in front of the centre of the specimen using an iron wire. With a TNT charge detonated in front of the pendulum face, the impulsive load produced by explosion would push the pendulum to translate. Based on the oscillation amplitude measured by a laser displacement transducer, the impulse transfer was further estimated. Another sensor known



(a) Ballistic pendulum system



(b) Clamping device

Fig. 1 Experimental setup

as PVDF pressure gauge was mounted at the centre of the specimen's front face to measure the pressure-time history. The complete process of explosion and loading was recorded using a high speed video camera.

3. FE model

The numerical simulation was implemented using the commercial FE package LS-DYNA 970/ explicit, which is suitable to handle the dynamic problems involving large deformation, high pressure/temperature/strain rate, failure of material, solid-fluid interaction etc. Detailed descriptions of the geometry, material, and boundary and loading conditions of the FE model are given in Sections 3.1, 3.2 and 3.3, respectively. Then the FE model is validated with a published analytical solution in Section 3.4.

3.1 Modelling geometry

The configuration of the square sandwich panel is shown in Fig. 2(a). The two face-sheets are bonded onto the honeycomb core, which consists of a 2D array of hexagonal cells. In the simulation, the mass per unit area of the structure, the area over which the blast loads are applied, and core thickness are fixed. Design variables include the thicknesses of the two face-sheets and relative density of core. Their effect on the deflection and failure modes of the structure is studied in detail; the influence of the pulse shape is also discussed. In the FE model, both the honeycomb core and face-sheets were modelled with Belytschko-Tsay shell elements (Hallquist 1998). The elements for a single cell (including the corresponding face-sheets) are illustrated in Fig. 2(b). The side length of each element is approximately 1.5 mm, and the entire model comprises 65, 696 shell elements. Convergence test was carried out for the mesh sizes to keep the results stable.

3.2 Modelling material

For simplicity, both the core and faces are assumed to be of the same material, Al-6005-T6. Its mechanical properties have been calibrated by Borvik *et al.* (2005): $E = 70$ GPa; $\nu = 0.3$; $\rho = 2700$

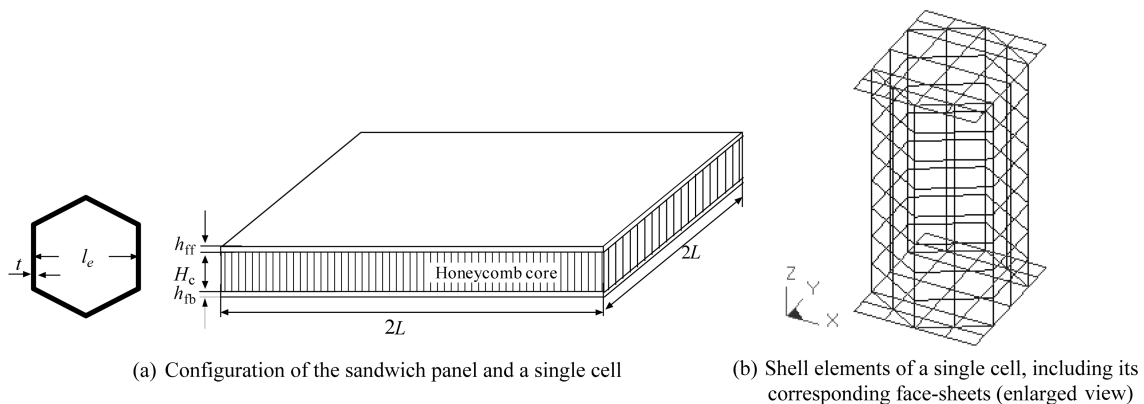


Fig. 2 Geometric model of the sandwich panel and a single honeycomb cell

kg/m³; $\sigma_Y = 270$ MPa. In the simulation, a simplified Johnson-Cook constitutive relationship (material model #99 in LS-DYNA) (Hallquist 1998) was used to describe its deformation and failure behaviours. Compared with the full J-C implementation (Johnson and Cook 1983), the simplified J-C model neglects material softening caused by high temperature; the dynamic flow stress of a material is expressed in a multiplicative form of strain and strain rate terms as

$$\sigma_{Yd} = (A + B\bar{\epsilon}^n)(1 + C \ln \dot{\epsilon}^*) \tag{1}$$

where A , B , and C are material constants, and n is work hardening exponent; $\bar{\epsilon}^p$ is effective plastic strain; $\dot{\epsilon}^* = \dot{\epsilon}/\dot{\epsilon}_0$, being the effective strain rate for $\dot{\epsilon}_0 = 1s^{-1}$. This model is suitable for problems where strain rates vary over a large range but without temperature effect. Damage at nodes begins when a tensile fracture strain (ϵ_f) is reached and after fracture is detected at all nodes of an element, that element is deleted from the further calculation. ϵ_f for Al-6005-T6 is taken as 0.363 (Borvik *et al.* 2005).

3.3 Modelling boundary and loading conditions

The square panels are fully fixed at the four edges, as shown in Fig. 3. Only a quarter of the structure was considered because of symmetry.

When an explosive charge is detonated in air, the rapidly expanding gaseous reaction products compress the surrounding air and move it outwards with a high velocity that is initially close to the detonation velocity of the explosive. The rapid expansion of the detonation products creates a shock wave (known as blast wave) with discontinuities in pressure density, temperature and velocity. The pressure-time history for a blast wave at a certain location is characterised by an exponential decay curve with peak pressure P_s and duration t_s , as shown in Fig. 4. In the present study, for simplicity, the blast load was idealised as a constant pressure with magnitude P_0 and pulse width t_0 , which is also shown in Fig. 4. The rectangular load is also known as effective pulse definition (Azevedo and

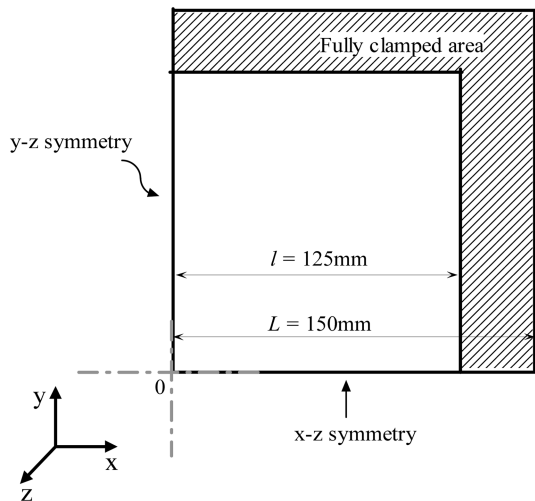


Fig. 3 Boundary conditions of the sandwich panel

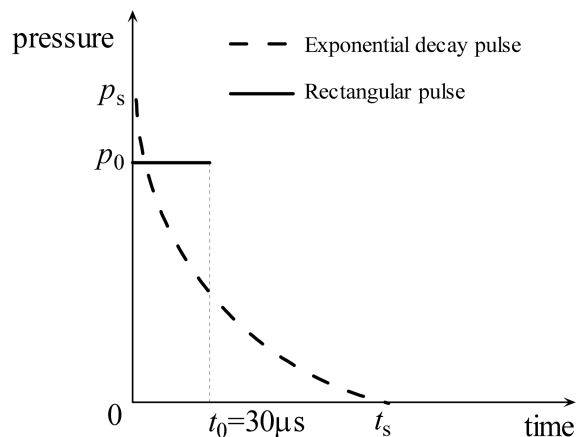


Fig. 4 Exponential decay and rectangular shock wave model

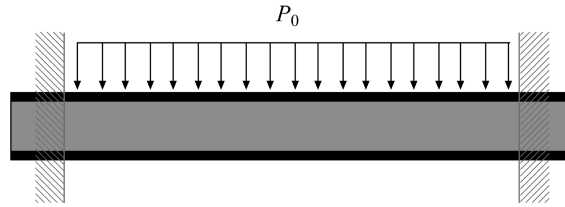


Fig. 5 Sketch of the uniform blast loading on a sandwich structure

Alves 2008), which is equivalent to the impulse of an arbitrary actual pulse. The effective values, involving only integrals of the loading, can significantly reduce the computing cost but give acceptable accuracy (Vaziri and Hutchinson 2007).

The pressure is applied on the front face of the sandwich panel. Therefore the impulse delivered onto the structure per unit area is $I_0 = P_0 t_0$. The uniform blast loading case is sketched in Fig. 5.

3.4 Model validation

The numerical simulation is validated by comparing its prediction of deflection with an analytical solution reported in (Zhu 2009a). The analytical model is based on an energy balance and assumed displacement fields. The maximum deflection at the back face of a square sandwich panel subjected to an impulse per unit area I_0 can be obtained by

$$\begin{cases} w_0 = \frac{A}{32} \cdot \frac{\bar{h} D_n}{(2\bar{h} + \bar{\rho})(H_c - h_f)} & w_0 \leq 2h_f + H_c \\ w_0 = \frac{1}{2\lambda} \sqrt{\frac{A \bar{h} D_n}{3.6(2\bar{h} + \bar{\rho})}} & w_0 > 2h_f + H_c \end{cases} \quad (2)$$

where $\bar{\rho} = \rho_c/\rho_f$ being the ratio of core mass density and face-sheet material density, equal to the relative density of the core; $\bar{h} = h_f/H_c$ being the thickness ratio of face-sheet and core, given that the two face-sheets are identical; A is the area of the plate exposed to the blast load; D_n is known as Johnson damage number (Johnson 1972), which has been widely used to assess the plastic response of a structure under dynamic or impulsive loading. It can be expressed in the following form:

$$D_n = \frac{I_0^2}{\rho_f \sigma_{Yd}^f h_f^2} \quad (3)$$

where σ_{Yd}^f is dynamic flow stress of the face-sheet material.

Here, the response of a typical sandwich panel is predicted by both the numerical and analytical models, and then the results are compared. Since the analytical solution is not able to describe damage, the centre deflection of back face is considered as the main response and the fracture of core and faces is neglected. The specification of the panel is as follows: $A = 0.0625 \text{ m}^2$; mass per unit area $M_0 = 5.36 \text{ kg/m}^2$; $h_f = 0.8125 \text{ mm}$; $H_c = 12.5 \text{ mm}$; $\bar{\rho} = 0.03$; both the face-sheets and core have the same base material, i.e., Al-6005-T6. The simulation and analytical predictions are compared and the result is shown in Fig. 6. The comparison is made by plotting normalised central point deflections ($\hat{w}_0 = w_0/l$) against normalised impulses per unit area ($\hat{I}_0 = I_0/(M_0 \sqrt{\sigma_{Yd}^f/\rho_f})$). The

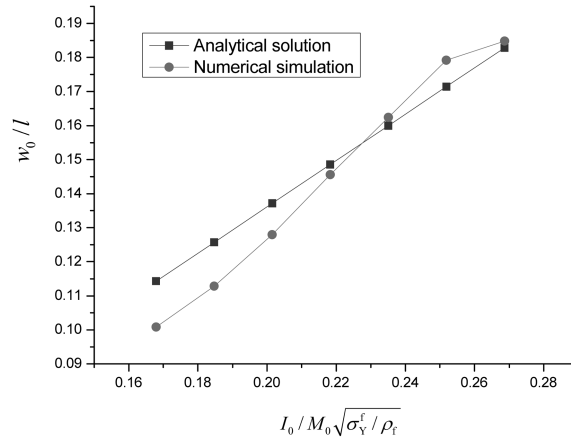


Fig. 6 Comparison of the numerically and analytically predicted centre deflection of the back face of a typical square sandwich plate ($A = 0.0625 \text{ m}^2$; $M_0 = 5.36 \text{ kg/m}^2$; $h_f = 0.8125 \text{ mm}$; $H_c = 12.5 \text{ mm}$; $\bar{\rho} = 3\%$)

result shows a reasonable agreement and it is clearly indicated that the numerical model gives reliable predictions of the sandwich panels' response to the uniform blast loads.

4. Uniform loading

The failure behaviour of monolithic structures under uniform blast loading has been studied by a number of researchers since 1970s. Three main failure modes were identified: (I) Large inelastic deformation; (II) Tearing (tensile failure) at or over the support; and (III) Transverse shear failure at the support. In each mode, more detailed failure patterns were further defined. Comprehensive reviews are available in (Jacob *et al.* 2007, Zhu and Lu 2007). In Sections 4 and 5, the failure criterion described in Section 3.2 is added into the material model to investigate the failure procedure and identify various damage modes of the sandwich structures.

4.1 General failure process of the sandwich panels

Under a uniformly distributed impulsive loading, the deformation and failure procedure of fully-clamped metallic sandwich panels are characterised by uniform core compression and face-sheets ductile tearing at supports. In the present context, core failure (mainly buckling) does not necessary imply its ultimate failure since a sandwich plate can still have substantial residual strength afterwards (Vaziri *et al.* 2007). Fig. 7 illustrates the deformation and failure process of a typical sandwich panel ($A = 0.0625 \text{ m}^2$; $M_0 = 5.36 \text{ kg/m}^2$; $H_c = 12.5 \text{ mm}$; $h_{ff} = h_{fb} = 0.875 \text{ mm}$; $\bar{\rho} = 2\%$) loaded by a normalised impulse per unit area $\bar{I}_0 = I_0 / (M_0 \sqrt{\sigma_Y^t / \rho_t}) = 0.37$. The whole failure process can be broadly divided into four consecutive phases:

- Phase I: Core crushing;
- Phase II: Front face tearing;
- Phase III: Back face tearing, while the core is still intact; and
- Phase IV: Structural full detachment, after the tearing of core.

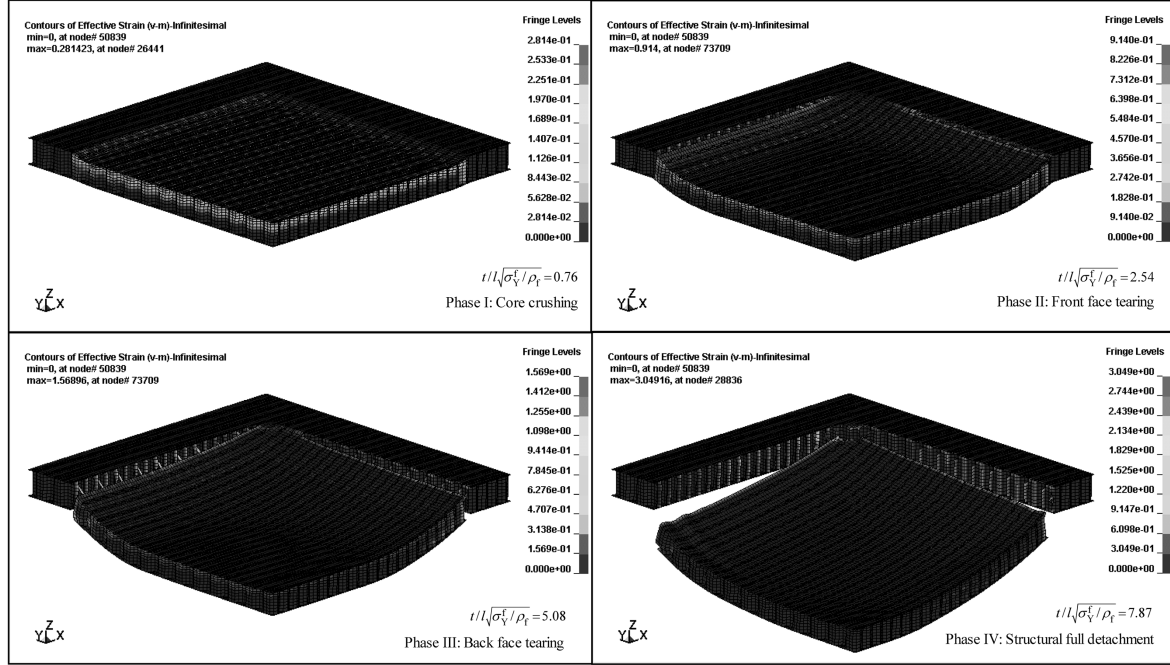


Fig. 7 Deformation and failure process of a typical sandwich panel ($A = 0.0625 \text{ m}^2$; $M_0 = 5.36 \text{ kg/m}^2$; $H_c = 12.5 \text{ mm}$; $h_{ff} = h_{fd} = 0.875 \text{ mm}$; $\bar{\rho} = 2\%$) subjected to a uniform blast loading

4.2 Failure modes

With various combinations of sandwich panel configurations and impulses applied, four deformation/failure modes can be identified, namely

- Mode 0 – The panel undergoes plastic deformation without face-sheets tearing. It has been suggested that when the maximum back face deflection of the sandwich structure is greater than its original panel thickness ($H_0 = h_{ff} + h_{fb} + H_c$), stretching plays a key role in the deformation mechanism and bending effect may be ignored; on the other hand, in the small deflection cases, bending dominates and the effect of stretching is negligible (Hutchinson and Xue 2005);
- Mode I – Only the front face tears but the back face and core remain intact;
- Mode II – Tearing takes place on both face-sheets; and
- Mode III – The structure fully detaches from the supports.

These modes are sketched in Fig. 8, where the cross-section of the sandwich plate is taken along the centre line and parallel to one edge. In this study, we use the deformation and failure modes to define the degrees of damage in the metallic sandwich structures: Mode 0: *preliminary damage*; Mode I: *intermediate damage*; Mode II: *severe damage*; Mode III: *critical damage*. The criterion may be somewhat subjective, but reasonable.

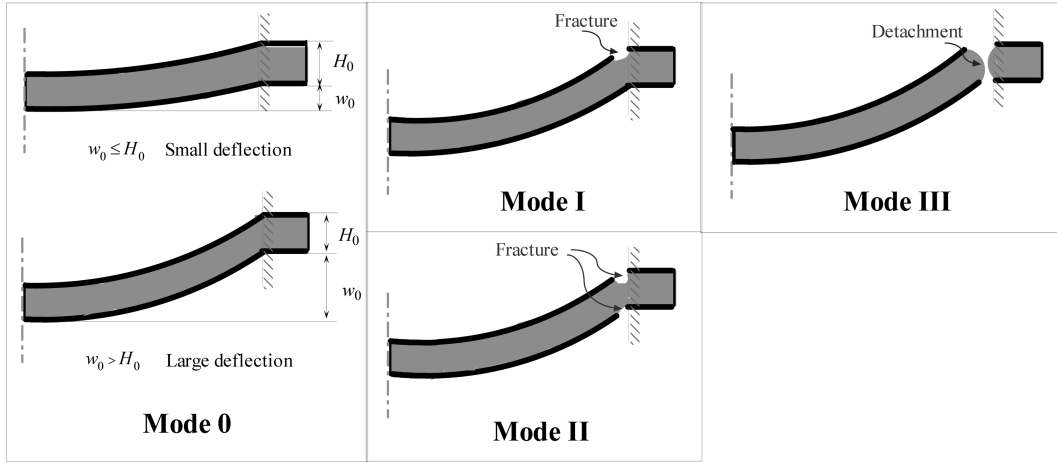


Fig. 8 Cross-sectional sketches of sandwich panels showing their failure modes

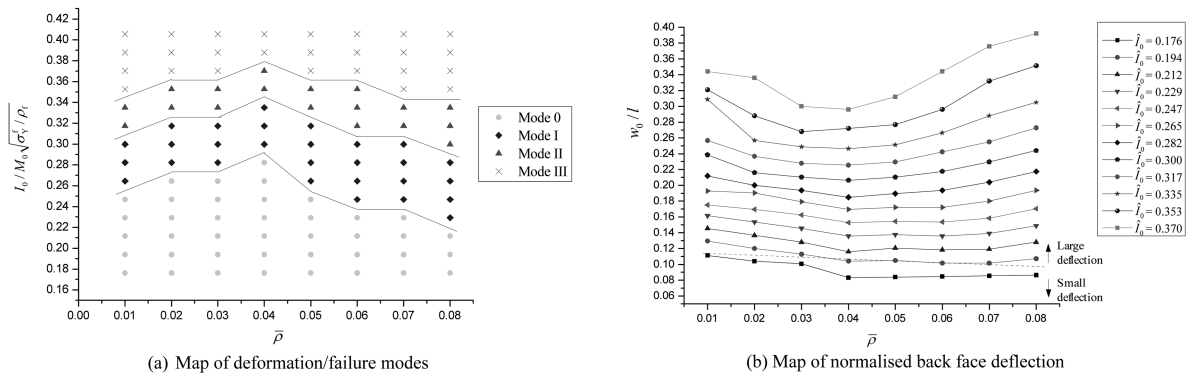


Fig. 9 Effect of core density under different levels of impulse ($M_0 = 5.36 \text{ kg/m}^2$; $A = 0.0625 \text{ m}^2$; $H_c = 12.5 \text{ mm}$; $\bar{\rho}$ ranges from 1% to 8%; \hat{I}_0 ranges from 0.176 to 0.370; Front and back faces are identical.)

4.3 Effect of core density

In this section, the effect of core density on the deformation/failure modes distribution is analysed. Fix the mass per unit area of the panel at 5.36 kg/m^2 , exposed area at $A = 0.0625 \text{ m}^2$ and the value of core thickness at 12.5 mm . The relative density of core varies from 1% to 8%, and the thickness of two identical face-sheets is reduced accordingly in order to keep the area per unit area constant. The panels were subjected to impulses ranging from $\hat{I}_0 = 0.176$ to $\hat{I}_0 = 0.370$. The distributions of failure modes and normalised back face deflections (w_0/l) are shown in Figs. 9(a) and 9(b), respectively.

The result shows that with increasing impulse, the failure mode of sandwich plates transfers from Mode 0 to Modes I, II and III consecutively. In Fig. 9(a), the sandwich panel with 4% core needs largest value of \hat{I}_0 for Modes I, II and III, and thus it offers the best performance against tearing. Similar result is obtained from Fig. 9(b), where the 4% core panel has the minimum back face deflection, in either the small or large deflection case. Using the map of deformation/failure modes

in Fig. 9(a), it is possible to establish the relationship between the ductility of face-sheet material and the maximum impulses for damage modes 0, I and II. For example, as for the panel with 4% core, let

$$\hat{I}_0 = \alpha \varepsilon_f \quad (4)$$

where α is equal to 0.78, 0.92 and 1.02 for Modes 0, I and II, respectively.

4.4 Effect of face thickness

Now consider the case of non-identical face-sheets. In this section, again, the mass per unit area and the area are kept unchanged, equal to 5.36 kg/m^2 and $A = 0.0625 \text{ m}^2$, respectively. $H_c = 12.5 \text{ mm}$ and $\bar{\rho} = 0.04$. The thickness ratio of the front and back faces (h_{ff}/h_{fb}) ranges from 1/9 and 9/1, and the structure is subjected to the same impulses ranging from 0.176 to 0.388. Figs. 10(a) and 10(b) indicate the failure modes and normalised back face deflections, respectively, under various combinations of \hat{I}_0 and $\bar{\rho}$.

In Fig. 10(a), as expected, the panels with thin front face ($h_{ff}/h_{fb} = 1/9, 2/8$ and $3/7$) are prone to Mode I early. But surprisingly, the thickest three front faces ($h_{ff}/h_{fb} = 7/3, 8/2$ and $9/1$) are relatively easy to tear, compared with the three front faces with medium thicknesses (i.e. $h_{ff}/h_{fb} = 6/4, 5/5$ and $4/6$), as it is conventionally presumed that thicker front face should be stronger. Also, the panels with almost two identical faces are the most reluctant to transfer from Mode I failure to Mode II. Mode III failure takes place on most of the sandwich panels almost at the same value of \hat{I}_0 . Fig. 10(b) shows that under low and medium levels of impulse ($\hat{I}_0 < 0.229$), the back face deflections of the panels with medium and thick front faces are very similar; those with thin front face deflect more dramatically. When the impulses become higher, structures with identical face-sheets have minimum displacements, and therefore can be considered as the optimal design.

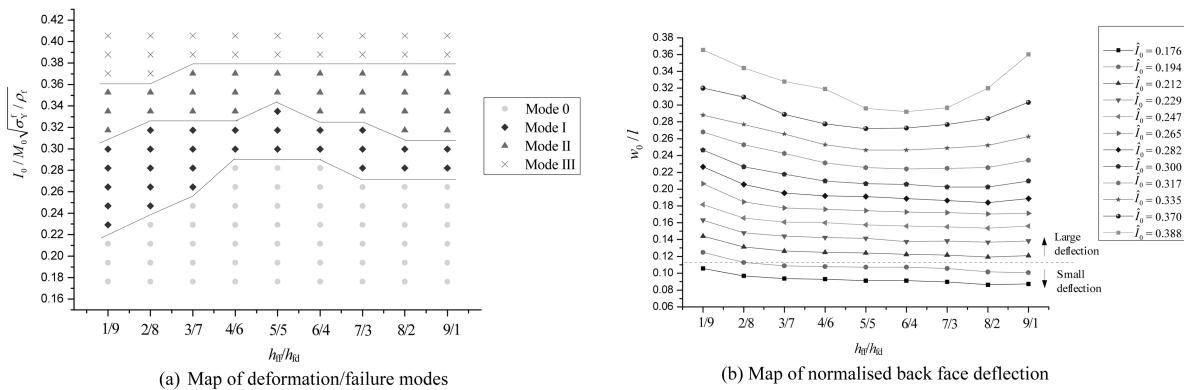


Fig. 10 Effect of front/back face thickness ratio under different levels of impulse ($M_0 = 5.36 \text{ kg/m}^2$; $A = 0.0625 \text{ m}^2$; $H_c = 12.5 \text{ mm}$; $\bar{\rho} = 4\%$; The thickness ratio (h_{ff}/h_{fb}) ranges from 1/9 and 9/1; \hat{I}_0 ranges from 0.176 to 0.388.)

4.5 Pressure-impulse characterisation

Sections 4.3 and 4.4 studied the effect of structural configurations (e.g., core density and thicknesses of face-sheets) of the sandwich panels on their response under blast loading. In this section, the influence of blast load history or shape of pulse, i.e. pressure-impulse characteristic, is discussed in detail using a commonly used analysis tool in the blast protective structures design, known as pressure-impulse (P-I) diagram. A P-I diagram is an iso-damage curve which allows the load-impulse combination that would cause a specified level of damage to be assessed very readily. Once a maximum displacement is defined (i.e., a damage criterion has been specified), this curve then indicates the pressure and impulse that would cause the failure of a particular structure subjected to a specified load. Combinations of pressure and impulse that fall to the left of and below the curve would not induce failure while those to the right and above the graph would produce damage in excess of the allowable limit (Smith and Hetherington 1994). This class of curve is actually equal energy curve predicting the degree of damage as a function of the physical parameters. The P-I diagrams have been applied in the blast protective areas to study structural damage criteria (Shi *et al.* 2008), effect of pulse shape (Li and Meng 2002) and the injuries of human organs (Baker *et al.* 1983).

It has been found that a strong relationship exists between the natural frequency of a structural component and the duration of the load. This relationship is normally categorised into three regimes: impulsive, quasi-static and dynamic, as shown in Fig. 11. In the impulsive loading regime, the loading duration is short relative to the system natural frequency. This forms a vertical asymptote that defines the minimum impulse required to reach a particular degree of damage, and the structure response is not sensitive to the peak pressure. For the quasi-static regime, on the contrary, the loading duration is significantly longer than the system natural frequency; the structural response can be assumed to be independent of the impulse, and a horizontal asymptote is used to quantify the minimum peak pressure which can cause a specified damage. The third transition regime, the dynamic regime, exists between the impulsive and quasi-static regions, where the response is more complex, and is greatly influenced by the load history.

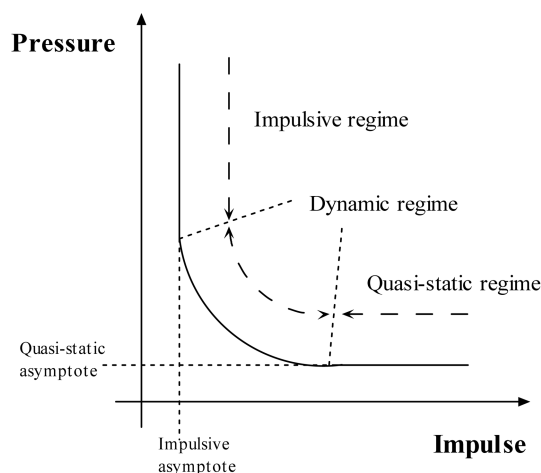


Fig. 11 Sketch of the P-I diagram

A P-I diagram can be developed using a single-degree-of-freedom (SDOF) system, with an energy solution (Smith and Hetherington 1994, Krauthammer 2008, Baker *et al.* 1983, Ma and Ye 2007, Ye and Ma 2007). A typical SDOF system may include mass, spring and dashpot, which represents inertia, resistance and damping, respectively. However, the use of SDOF model may not be suitable for structure damage analysis to intense blast loads, as such approach can neither describe the structural damage in detail, nor identify different failure modes (Shi *et al.* 2008). On the other hand, using physical tests to generate the data points for P-I diagram is quite expensive. Therefore, it is an economic and effective way to use numerical simulation to obtain a sufficient number of computed points to establish P-I curves, assuming that the problem is accurately modelled.

To date, no P-I diagrams for sandwich structures to shock loads have been reported. In the following sub-sections, we shall investigate the pressure-impulse characterisation of a typical square sandwich panel with the following specification: $A = 0.0625 \text{ m}^2$; $M_0 = 5.36 \text{ kg/m}^2$; $h_{ff} = h_{fb} = h_f = 0.75 \text{ mm}$; $H_c = 12.5 \text{ m}$; $\bar{\rho} = 0.04$.

4.5.1 Determination of the pressure and impulse asymptotes

Before a P-I diagram is obtained, its pressure and impulse asymptotes should be determined first, which can significantly narrow the scope of subsequent search of the data points, and thus can reduce the computational cost. Here, a simple analytical analysis is proposed to estimate these two asymptotes.

Fleck and co-workers (Fleck and Deshpande 2004, Qiu *et al.* 2004) theoretically investigated the response of sandwich structures loaded by blasts without damage. The complete deformation process *before* the front face-sheet tears (Mode I) has been split into three stages:

- Stage I : Blast impulse is transmitted to the front face of sandwich structure, and the front face would instantly attain a velocity v_1 while the rest of the structure is stationary.
- Stage II : The core is compressed while the back face is stationary.
- Stage III: The back face starts to deform and finally the structure is brought to rest by plastic bending and stretching.

Given the impulse delivered on the front face (I), with the impulse transmission, the front face obtains an initial velocity

$$v_1 = \frac{I}{A\rho_f h_f} \quad (5)$$

Then the initial kinetic energy of the front face is calculated by Eq. (6), which is also the total energy of the structure obtained from the blast load

$$W_1 = \frac{I^2}{2A\rho_f h_f} \quad (6)$$

At the end of Stage II, the whole structure would have an identical velocity, and the kinetic energy per unit area can be calculated by

$$W_{II} = \frac{I^2}{2A(2\rho_f h_f + H_c \rho_c)} \quad (7)$$

The energy loss should be fully dissipated during core crushing. Then the residual kinetic energy at the end of Stage II (W_{II}) is dissipated by plastic bending and stretching of the panel in Stage III.

According to the simulation results in Section 4.3, the maximum deflections of all the panels at the interface of Mode 0 and Mode I failure are greater than their original thickness (i.e., $w_0 < 2h_f + H_c$), and bending effect can be neglected and large deflection theory should be applied. Following conventional large deflection analysis (Timoshenko 1959) of a square plate, under a uniformly distributed impulsive loading, its final deflection distribution is assumed by the following equation

$$w = w_0 \cos \frac{\pi x}{2l} \cos \frac{\pi y}{2l} \quad (8)$$

with w_0 being the permanent deflection at the centre point. For simplicity, the front face and the back face are assumed to have the same profile. Based on the approach proposed in (Zhu *et al.* 2009a), the energy dissipated during plastic stretching (U_s) can be expressed as

$$\begin{aligned} U_s &= 2h_f \times 4 \int_0^l \int_0^l \left(\sigma_{Yd}^f (\varepsilon_x + \varepsilon_y) + \frac{\sigma_Y^f}{\sqrt{3}} \gamma_{xy} \right) dx dy \\ &= 7.25 w_0^2 \sigma_{Yd}^f h_f \end{aligned} \quad (9)$$

with ε_x , ε_y and γ_{xy} being the in-plane strain components of face-sheets, which can be derived from Eq. 8. In the present case, since the in-plane tensile strength of the hexagonal cells is very small, their contribution to the stretching dissipation is ignored (Qiu *et al.* 2004). Equating W_{II} and U_s yields

$$\frac{I_{cr}^2}{2(2\rho_f h_f + H_c \rho_c)} = 7.25 w_{cr}^2 \sigma_{Yd}^f h_f \quad (10)$$

where w_{cr} is the critical deflection beyond which tearing would happen on the front face; I_{cr} is the corresponding critical impulse. The critical deflection of the panel concerned was obtained from the numerical simulation in Section 4.3, i.e., $w_{cr} = 0.023$ m. Then the critical impulse is solved: $I_{cr} = 22.9$ Ns. Its normalised value ($\hat{I}_{cr} = I_{cr} / (AM_0 \sqrt{\sigma_Y^f / \rho_f}) = 0.22$) is taken as the impulse asymptote.

On the other hand, in the quasi-static loading case, with the same profile as that under the impulsive condition, the strain energy of the structure after core compression (U_s) should be equal to the work done by the external pressure (W_p), i.e.

$$W_p = U_s = 4P_{cr} \int_0^l \int_0^l w_{cr} \cos \frac{\pi x}{2l} \cos \frac{\pi y}{2l} dx dy \quad (11)$$

where P_{cr} is the critical pressure which is the minimum pressure required to cause the front face tearing. Substituting $w_{cr} = 0.023$ m into Eq. (11) gives $P_{cr} = 1.3$ MPa. The corresponding normalised value ($\hat{P}_{cr} = (P_{cr} / \sigma_Y^f) \times 10^3 = 4.8$) is the quasi-static asymptote. It should be noted that under the quasi-static loading condition, the static yield strength (σ_Y^f), rather than the dynamic flow stress (σ_{Yd}^f) is used to calculate the stretching dissipation (U_s).

4.5.2 Generation of the P-I diagram

The vertical and horizontal asymptotes obtained above are employed as the lower bounds of the impulse and pressure which will cause damage. Then numerical simulations are conducted to obtain the damage degrees for the sandwich plates loaded by various combinations of impulse and

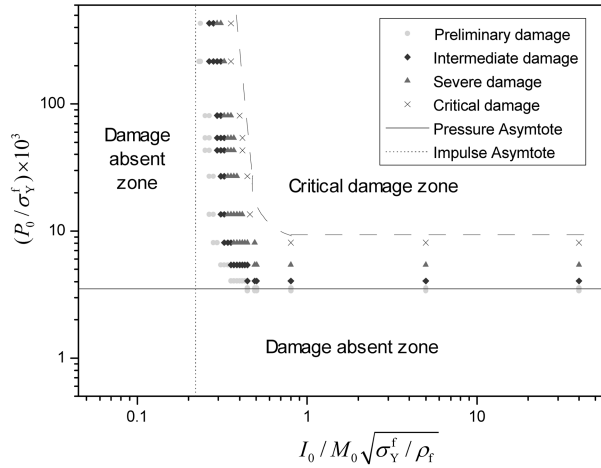


Fig. 12 P-I diagram for a sandwich panel with $A = 0.0625 \text{ m}^2$; $M_0 = 5.36 \text{ kg/m}^2$; $h_f = 0.75 \text{ mm}$; $H_c = 12.5 \text{ mm}$; $\bar{\rho} = 0.04$

pressure, and the data points are plotted with proper symbols in the P-I space. Fig. 12 shows the resultant P-I diagram.

5. Localised loading

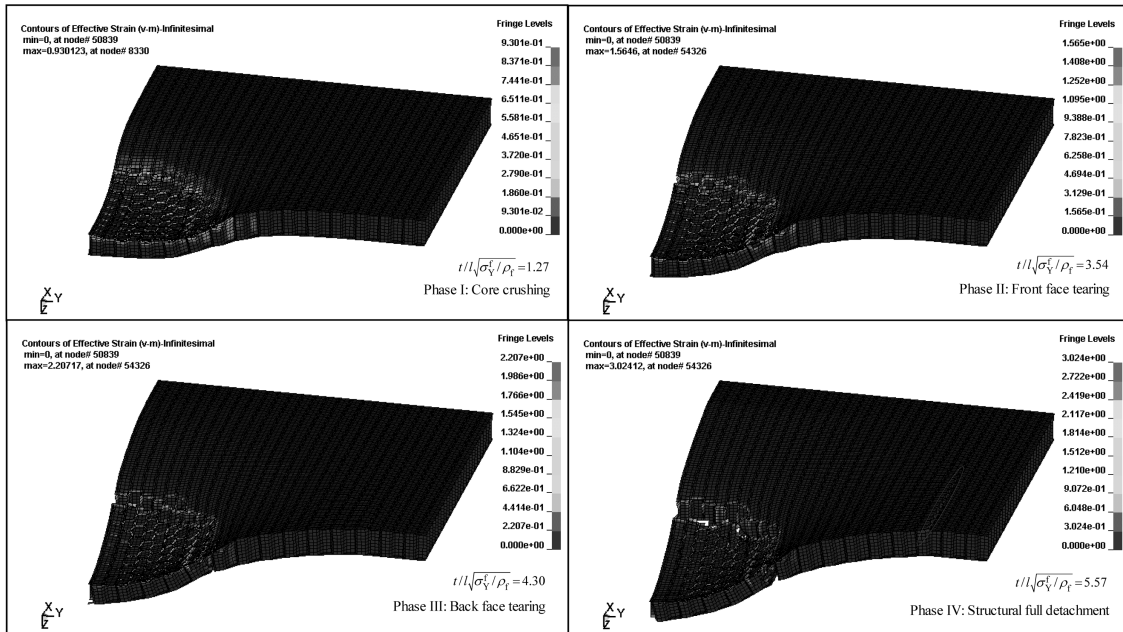
In this section, failure modes of sandwich panels subjected to localised blast loading are analysed. First, the deformation/failure process and modes of a typical sandwich plate loaded in the central area are presented; then a comparative study is conducted to evaluate the localised blasting resistant performances of a sandwich panel with honeycomb core, two face-sheets with air core and a monolithic plate, which have the same material and identical mass per unit area, in terms of their maximum deflections and failure behaviours.

5.1 General failure process and modes of the sandwich panels

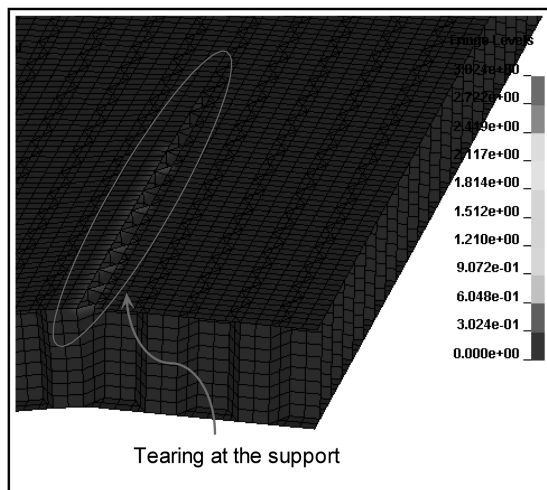
The failure procedure and modes for locally loaded sandwich structures are similar to those observed for uniformly loaded plates. The main difference is an additional capping damage, that is, tearing of a central fragment, or ‘cap’ (Nurick and Radford 1997, Langdon *et al.* 2005). As an example, a typical sandwich plate is considered here, which has the following configuration: $A = 0.0625 \text{ m}^2$; $M_0 = 5.36 \text{ kg/m}^2$; $h_f = 0.0625 \text{ mm}$; $H_c = 12.5 \text{ mm}$; $\bar{\rho} = 0.06$. The load is applied in a circular area (radius $r = l/2 = 62.5 \text{ mm}$) at the central portion of the square plate, with the time duration $t_0 = 30 \text{ } \mu\text{s}$. The peak pressure $P_0 = 45 \text{ MPa}$, having a uniform distribution over the loaded region, i.e.

$$\begin{cases} P(r) = P_0 & \text{for } 0 \leq r \leq l/2 \\ P(r) = 0 & \text{for } l/2 < r \leq l \end{cases} \quad (12)$$

Fig. 13(a) illustrates the general deformation and failure process of the sandwich panel. With the



(a) Failure procedure



(b) Tearing of the front face-sheet at the support

Fig. 13 Deformation and failure process of a typical sandwich plate ($A = 0.0625 \text{ m}^2$; $M_0 = 5.36 \text{ kg/m}^2$; $h_f = 0.625 \text{ mm}$; $H_c = 12.5 \text{ mm}$; $\bar{\rho} = 6\%$) subjected to a localised blast loading

impulse applied on the central portion, the front face at the area under loading starts to deflect, then followed by a localised core compression, which is much more significant than in the uniform loading case. After that, the back face deforms, and tearing failure takes place on the front face along the circular boundary of the loaded area. Next, the back face and core tear consecutively. Finally, the central fragment fully detaches from the structure. Tearing failure can also be observed at the outside boundary near the supports, as shown in Fig. 13(b).

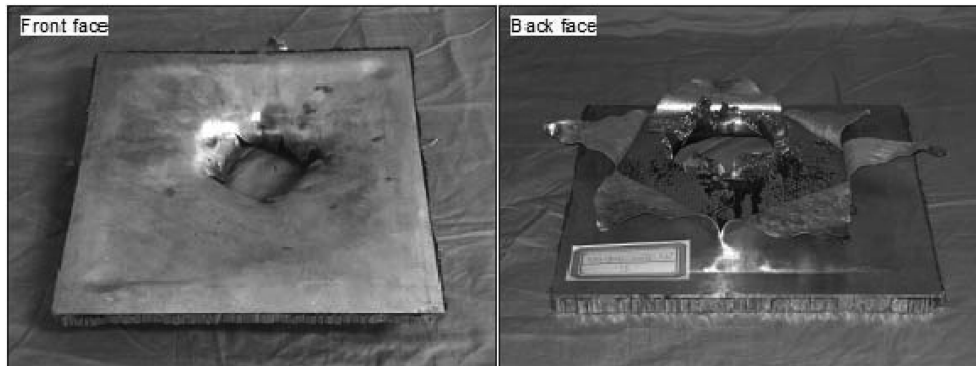


Fig. 14 Petalling damage of a sandwich panel ($A = 0.0625 \text{ m}^2$; $h_f = 0.625 \text{ mm}$; $H_c = 12.5 \text{ mm}$; $\bar{\rho} = 2.5\%$)

When the impulse is sufficiently large, the plate tears in a ‘petalling’ fashion. That is, tearing at centre with ‘petals’ of material folds away from the blast location (Nurick and Radford 1997). Fig. 14 shows the photographs of the petalling damage pattern of a typical sandwich panel obtained in our blast tests.

5.2 Comparative study

Comparative studies have been carried out for the blast resistant behaviours of sandwich and monolithic structures subjected to uniform shock loads. It has been shown that under the air blast loading, when the impulse is relatively small, sandwich structures have superior blast resistance (with smaller back face deflections) than solid structures; while under large impulsive loading, solid structures exhibit better performance (Xue and Hutchinson 2003, 2004, Hutchinson and Xue 2005). To date, no such analysis is available on the localised blast loading.

In this research, a comparison is made among three structures loaded locally: sandwich panel with honeycomb core (denoted SH), two face-sheets with air core (denoted FA) and monolithic plate (denoted MP). They have the material, area and mass mentioned in the above sections; the other specifications are shown in Fig. 15.

The failure modes of locally loaded monolithic plates (MP) have been well investigated experimentally and numerically (Nurick and Radford 1997, Langdon *et al.* 2005). A plate

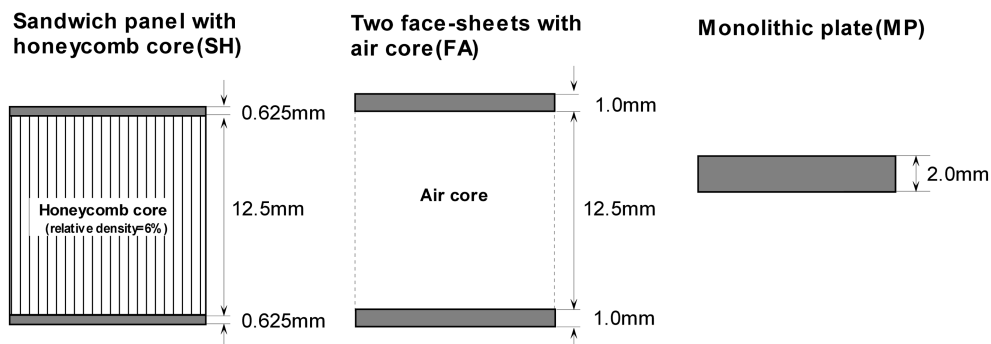


Fig. 15 Configurations of the three types of structures: sandwich panel with honeycomb core (SH), two face-sheets with air core (FA) and monolithic plate (MP)

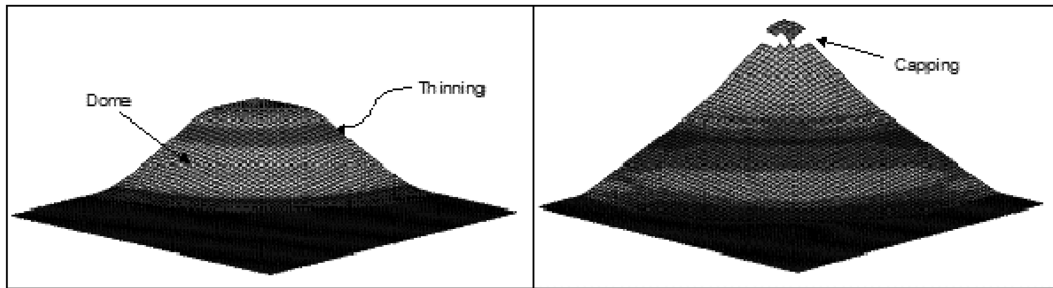


Fig. 16 Failure modes of a monolithic plate (MP structure) under localised blast loading

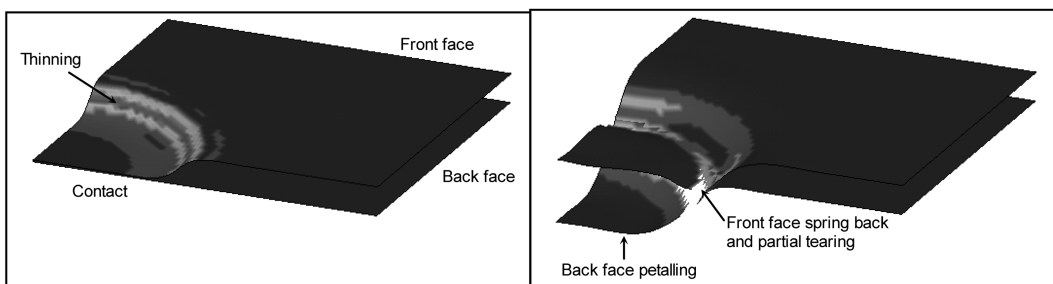


Fig. 17 Failure modes of two face-sheets with air core (FA structure) under localised blast loading

demonstrates large plastic deformation in a shape of a uniform circular dome. At higher impulses, a circular ring of thinning can be observed in the central region of the plate followed by partial tearing in the central portion and complete tearing as impulse continues increasing. The thinning and capping modes are illustrated in Fig. 16.

Compared with the MP structures, the FA structures have a much more complex deformation mechanism, as the interaction of the two face-sheets is involved. With the impulse applied, the front face deflects and then contacts with the back face; the back face starts to deform and the front face springs back in the mean time. If the impulse is sufficiently large, the back face would fracture first, followed by the front face, both at the central circular boundary, as shown in Fig. 17.

To make a comparison among the three different types of structures, a uniform criterion is set to assess their damage degrees under localised blast loading:

Preliminary damage:	Plastic deformation without face tearing
Intermediate damage:	Tearing of one face-sheet with the other one intact
Severe damage:	Tearing of both face-sheets
Critical damage:	Detachment of central portion

As an MP structure has only one face-sheet, its capping failure mode may be deemed as severe damage, and the petalling failure mode corresponds to critical damage. Fig. 18 shows the distributions of deflections and damage degrees of the three structures loaded by impulses (\hat{I}_0) ranging from 0.18 to 1.15. The deflections under intermediate, severe and critical damages are taken at the instant just before the damage happening. For SH and FA structures, only back face deflections are considered.

The result reveals similar trends for the three types of structures. The damage modes transmit

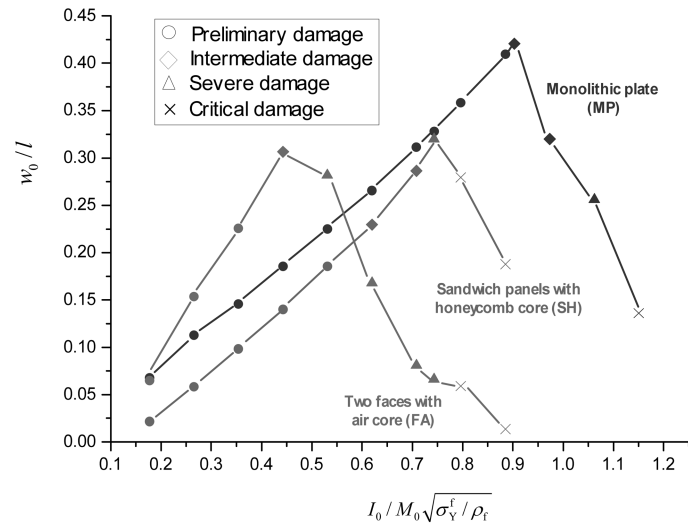


Fig. 18 Distributions of the deflections and damage degrees of the three types of structures (SH, FA and MP) under localised blast loading

from ‘preliminary’ to ‘critical’ damage consecutively with the impulse increasing. However, the centre point deflection decreases as impulse is increased beyond the threshold of intermediate damage, as the failure tends towards large shear at the outside boundary edge, which has been observed in the blast tests for the solid mild steel plates (Jacob *et al.* 2007). Compared with MP and SH structures, the FA structure has the largest permanent deformation for the same impulses, and is the earliest to fail and collapse. Thus, one can conclude that FA structure has the worst blast resistant performance among the three structures. At low impulses, the SH structure has smaller deflections than MP structure, which represents a better performance. When the impulse is increased to approximately 0.75, they have almost identical deflections. After that, the SH structure collapses quickly, while the MP structure continues deflecting. Therefore, it is concluded that MP structure has a superior shock resistance than the SH counterpart at high impulse levels. This finding is similar to that for the uniform loading case.

6. Conclusions

A numerical simulation study has been conducted to investigate the failure behaviour of square metallic sandwich panels under either uniform or localised blast loading. Both the honeycomb core and face-sheets were modelled with shell elements. For simplicity, they were assumed to have the same base material; the material properties were taken from the published literature and modelled using a simplified Johnson-Cook constitutive equation, where the strain and strain rate hardening effects have been considered but the temperature softening was disregarded. The shock load was idealised as a pressure over a short time. The FE model was validated by comparing its prediction of the sandwiches’ back face deflections with an analytical solution, and the result shows a reasonable agreement. Using the numerical model, the failure process of sandwich plates was studied, which includes four consecutive phases: (1) core crushing; (2) front face tearing; (3) back face tearing; and (4) structural full detachment. Then four distinct failure modes were identified

accordingly: Mode 0 – The panel undergoes plastic deformation without face-sheets tearing; Mode I – The front face tears but the back face keeps intact; Mode II – Tearing takes place on both face-sheets; and Mode III – The structure fully detaches from the supports. In the uniform loading case, based on the failure modes defined, the effect of core density and the front face/back face thickness ratio on the failure modes distribution was then analysed, with the mass per unit area of the sandwich plate, the area exposed to the loads and thickness of the core fixed. It has been found that the panel with core relative density of 4% and identical face-sheets has the best performance. Likewise, the influence of magnitude and duration of the blast loading on the failure modes was investigated by deriving a pressure-impulse (P-I) diagram. A simple analytical model was developed to determine the lower bounds of the pressure and impulse which would cause failure in the P-I space. Localised loading leads to similar failure modes to those observed for uniformly loaded plates. The main differences are much more significant core crushing in the loaded area and an additional tearing pattern of a central flake. Finally, a comparative study is carried out for the blast resistant behaviours of three types of structures loaded locally: sandwich panel with honeycomb core (SH), two face-sheets with air core (FA) and monolithic plate (MP). It has been shown that FA structure has the worst performance. Likewise, when the impulse is relatively small, SH has superior blast resistance than MP structure; otherwise, MP structure exhibits better performance.

Acknowledgements

The reported research is financially supported by the Australian Research Council (ARC) through a Discovery Grant, which is gratefully acknowledged.

References

- Abrate, S. (1989), *Impact on Composite Structures*, Cambridge University Press, Cambridge, UK.
- Azevedo, R.L. and Alves, M. (2008), "A numerical investigation on the visco-plastic response of structures to different pulse loading shapes", *Eng. Struct.*, **30**, 258-267.
- Baker, W.E., Cox, P.A., Westine, P.S., Kulesz, J.J. and Strehlow, R.A. (1983), *Explosion Hazards and Evaluation*, Elsevier, London, UK.
- Borvik, T., Clausen, A.H., Eriksson, M., Berstad, T., Hopperstad, O.S. and Langseth, M. (2005), "Experimental and numerical study on the perforation of AA6005-T6 panels", *Int. J. Impact Eng.*, **32**, 35-64.
- Dharmasena, K.P., Wadley, H.N.G., Xue, Z. and Hutchinson, J.W. (2008), "Mechanical response of metallic honeycomb sandwich panel structures to high-intensity dynamic loading", *Int. J. Impact Eng.*, **35**(9), 1063-1074.
- Fleck, N.A. and Deshpande, V.S. (2004), "The resistance of clamped sandwich beams to shock loading", *J. Appl. Mech.*, ASME, **71**, 386-401.
- Hallquist, J.O. (1998), *LS-DYNA Theoretical Manual*. Livermore, Livermore Software Technology Co., Livermore, CA, USA.
- Hutchinson, J.W. and Xue, Z. (2005), "Metal sandwich plates optimized for pressure impulses", *Int. J. Mech. Sci.*, **47**, 345-569.
- Jacob, N., Nurick, G.N. and Langdon, G.S. (2007), "The effect of stand-off distance on the failure of fully clamped circular mild steel plates subjected to blast loads", *Eng. Struct.*, **29**, 2723-2736.
- Johnson, G.R. and Cook, W.H. (1983), "A constitutive model and data for metals subjected to large strain rates and high temperatures", *Proceeding of 7th International Symposium on Ballistics*, Hague, the Netherlands.
- Johnson, W. (1972), *Impact Strength of Materials*, Edward Arnold, London, UK.

- Krauthammer, T. (2008), *Modern Protective Structures*, CRC, Abingdon, USA.
- Langdon, G.S., Yuen, S.C.K. and Nurick, G.N. (2005), "Experimental and numerical studies on the response of quadrangular stiffened plates. Part II: Localised blast loading", *Int. J. Impact Eng.*, **31**, 85-111.
- Li, Q.M. and Meng, H. (2002), "Pulse loading shape effects on pressure-impulse diagram of an elastic-plastic, single-degree-of-freedom structural model", *Int. J. Mech. Sci.*, **44**, 1985-1998.
- Lu, G. and Yu, T.X. (2003), *Energy Absorption of Structures and Materials*, Woodhead Publishing Ltd., Cambridge, UK.
- Ma, G.W. and Ye, Z.Q. (2007), "Analysis of foam claddings for blast alleviation", *Int. J. Impact Eng.*, **34**(1), 60-70.
- Nurick, G.N. and Radford, A.M. (1997), "Deformation and tearing of clamped circular plates subjected to localised central blast loads", *Recent Developments in Computational and Applied Mechanics, a Volume in Honour of John B. Martin*, Barcelona: CIMNE.
- Qiu, X., Deshpande, V.S. and Fleck, N.A. (2003), "Finite element analysis of the dynamic response of clamped sandwich beams subject to shock loading", *Euro. J. Mech. A/Solids*, **32**, 801-814.
- Qiu, X., Deshpande, V.S. and Fleck, N.A. (2004), "Dynamic response of a clamped circular sandwich plate subject to shock loading", *J. Appl. Mech.*, ASME, **71**, 637-645.
- Shi, Y., Hao, H. and Li, Z.X. (2008), "Numerical derivation of the pressure-impulse diagrams for prediction of RC column damage to blast loads", *Int. J. Impact Eng.*, **35**, 1213-1227.
- Smith, P.D. and Hetherington, J.G. (1994), *Blast and Ballistic Loading of Structures*, Butterworth-Heinemann, Oxford, UK.
- Timoshenko, S. (1959), *Theory of Plates and Shells*, McGraw-Hill, New York, USA.
- Vaziri, A. and Hutchinson, J.W. (2007), "Metal sandwich plates subject to intense air shocks", *Int. J. Solids Struct.*, **44**, 2021-2035.
- Vaziri, A., Xue, Z. and Hutchinson, J.W. (2007), "Performance and failure of metal sandwich plates subjected to shock loading", *J. Mech. Struct.*, **2**, 101-117.
- Xue, Z. and Hutchinson, J.W. (2003), "Preliminary assessment of sandwich plates subject to blast loads", *Int. J. Mech. Sci.*, **45**, 687-705.
- Xue, Z. and Hutchinson, J.W. (2004), "A comparative study of impulse-resistant metal sandwich plates", *Int. J. Impact Eng.*, **30**, 1283-1305.
- Ye, Z.Q. and Ma, G.W. (2007), "Effects of foam claddings for structure protection against blast loads", *J. Eng. Mech.*, ASCE, **133**(1), 41-47.
- Zhu, F. and Lu, G. (2007), "A review of blast and impact of metallic and sandwich structures", *Electronic J. Struct. Eng.*, Special Issue, 92-101.
- Zhu, F., Zhao, L.M., Lu, G. and Wang, Z. (2008a), "Deformation and failure of blast-loaded metallic sandwich panels — Experimental investigations", *Int. J. Impact Eng.*, **35**, 937-951.
- Zhu, F., Zhao, L.M., Lu, G. and Wang, Z. (2008b), "Structural response and energy absorption of sandwich panels with an aluminium foam core under blast loading", *Adv. Struct. Eng.*, **11**(5), 525-536.
- Zhu, F., Wang, Z., Lu, G. and Zhao, L.M. (2009a), "Analytical investigation and optimal design of sandwich panels subjected to shock loading", *Mater. Des.*, **30**, 91-100.
- Zhu, F., Zhao, L.M., Lu, G. and Gad, E. (2009b), "A numerical simulation on the blast impact of square metallic sandwich panels", *Int. J. Impact Eng.*, in press.
- Zhu, F., Wang, Z., Lu, G. and Nurick, G.N. (2009c), "Theoretical considerations on the dynamic response of sandwich structures under impulsive loading", Submitted for publication.